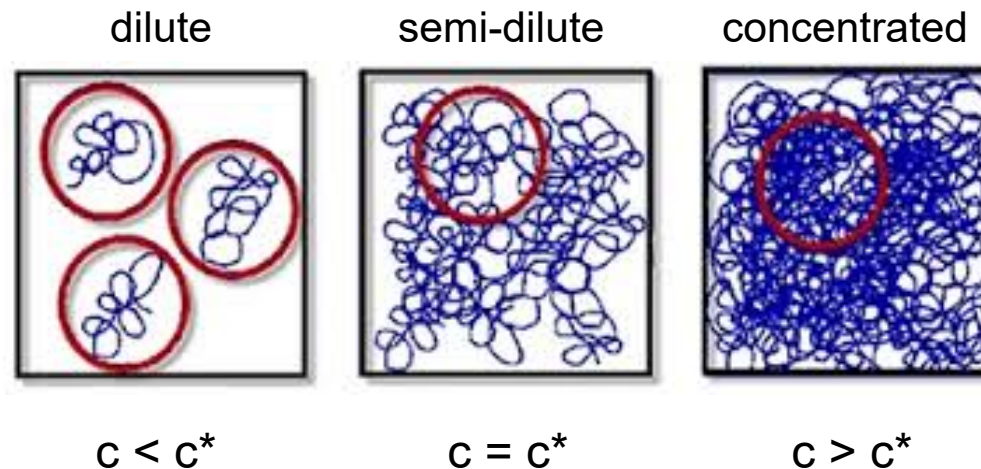


Concentrated Solution, Phase Separation Behavior



c^* : coil overlap concentration

Introduction

Dilute solutions were required for:

Determination of average molecular weights
Determination of sizes and forms

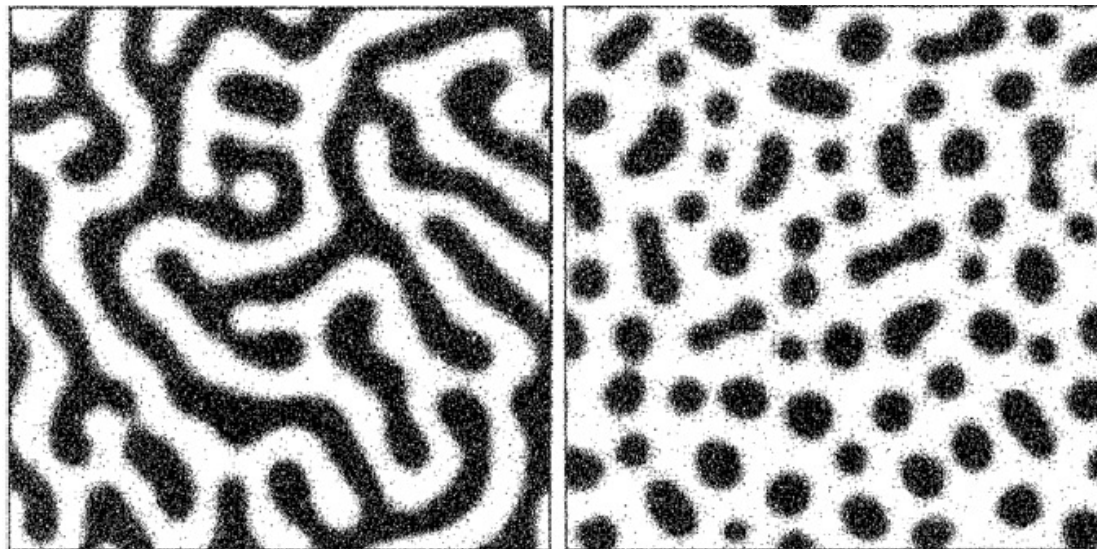
A wide range of modern research as well as a variety of engineering applications exist for polymer solution, but not diluted.

TABLE 4.1 Selected Industrial Applications of Polymer Solutions and Precipitates

Polymer	Solvent	Effect	Application
Sodium carboxymethyl cellulose	Soapy water	Selective precipitation onto clothing fibers	Prevents oils from redepositing on clothing during detergent washing; antiredeposition agent
Diblock copolymers	Motor oil	Colloidal suspensions dissolve at high temperatures, raising viscosity	Multiviscosity (constant viscosity) motor oil, Example: 10W-40
Poly(ethylene oxide) $M = 10^6$ g/mol	Water	Reduces turbulent flow	Heat exchange systems, reduces pumping costs
Proteins	Wine	Gels on reacting with tannin	Clarification of wines, removes colloidal matter
Polystyrene, various	Triglyceride oils	Viscosity control, phase-separates during oil polymerization	Oil-based house paints, makes coatings harder, tougher
Polyurethanes, various cellulose esters	Esters, alcohols, various	Solvent vehicle evaporates, leaving polymer film for glues, solvent enters mating surfaces	Varnishes, shellac, and glues (adhesives)
Poly(vinyl chloride)	Dibutyl phthalate	Plasticizes polymer	Lower polymer T_g , softens polymer, makes "vinyl"
Polystyrene	Poly(2,6-dimethyl-1,4-phenylene oxide)	Mutual solution; toughens polystyrene	Impact-resistant objects, such as appliances
Poly(methyl methacrylate)	Poly(vinylidene fluoride)	Increases PMMA oil and solvent resistance	Automotive applications parts that might contact gasoline

Introduction

Why do we care?



spinodal decomposition

binodal decomposition

Outline

Phase Separation:

Phase Diagram of Polymer – Solvent Systems

Measuring Phase Diagrams

Fractionation

Phase Diagram of Polymer – Polymer Systems

Kinetic of Phase Separation:

Nucleation and Growth

Spinodal Decomposition

Annexe:

Block Copolymers Phase Behaviour

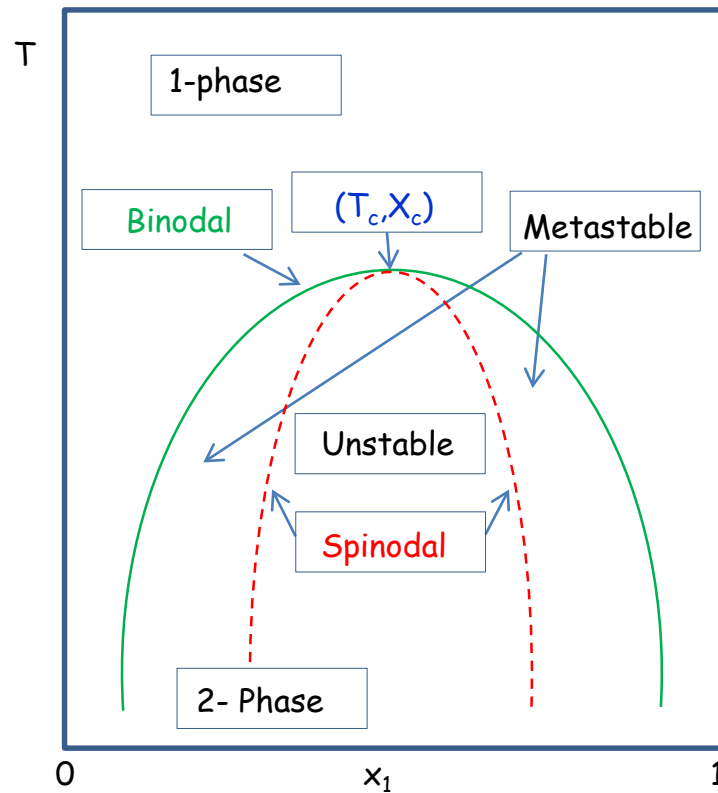
Phase Diagram of Binary Systems

Phase diagram for regular solution theory (T versus mole fraction of comp. 1)

Binodal (Coexistence curve): separating the **one-phase** region at high T from the **two-phase** region at low T

Spinodal: (Stability limit): separating the **unstable** and **metastable** windows within the two-phase region.

Critical Point: Meeting of binodal and spinodal curves

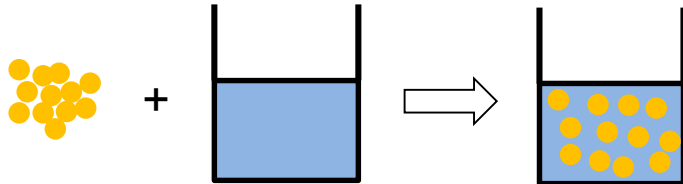


Phase separation will occur whenever the system can **lower** its total free energy by dividing into two phases.

Review: Change in Entropy and Enthalpy

entropy

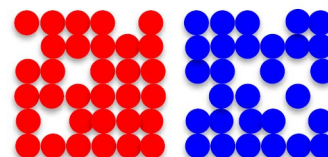
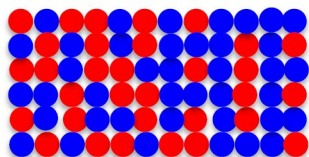
$$\Delta S_m = -R(x_1 \ln x_1 + x_2 \ln x_2)$$



Assumption: The probability for the nearest neighbor of A to be A is equal to that of the nearest neighbor of A to be B.

enthalpy

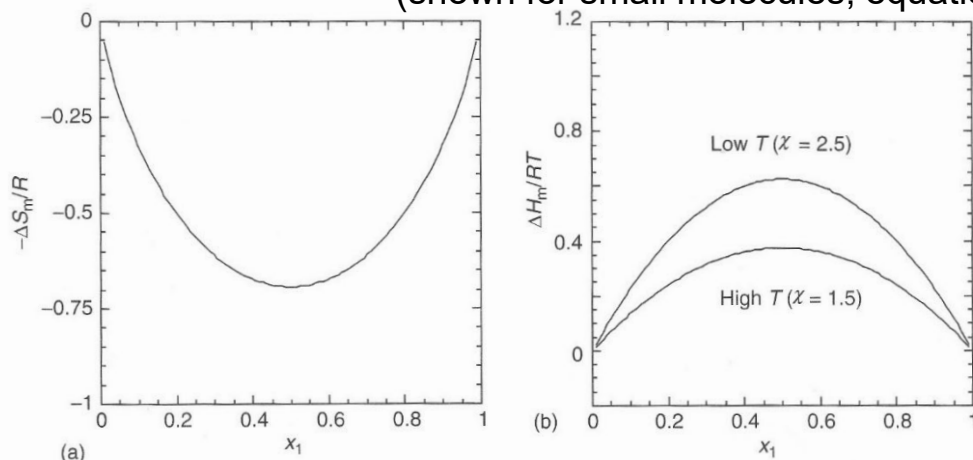
$$\Delta H_m = \frac{z}{2} \underbrace{(v_1^2 w_{11} + v_2^2 w_{22} + 2v_1 v_2 w_{12})}_{H_{12}} - \frac{z}{2} \underbrace{(v_1 w_{11} + v_2 w_{22})}_{H_1 + H_2}$$



Assumption: no volume change upon mixing

Predictions of Regular Solution Theory

(shown for small molecules, equation given per mole)



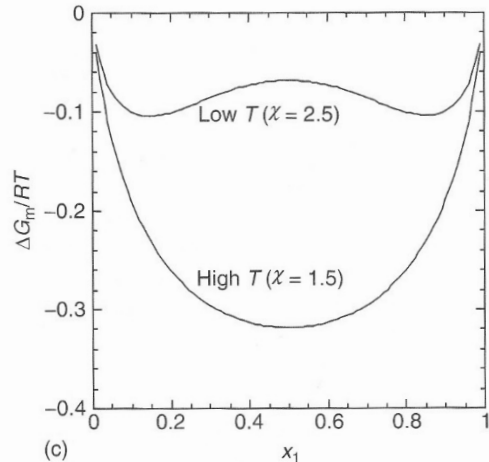
$$-\frac{\Delta S_m}{R} = x_1 \ln x_1 + x_2 \ln x_2$$

entropy

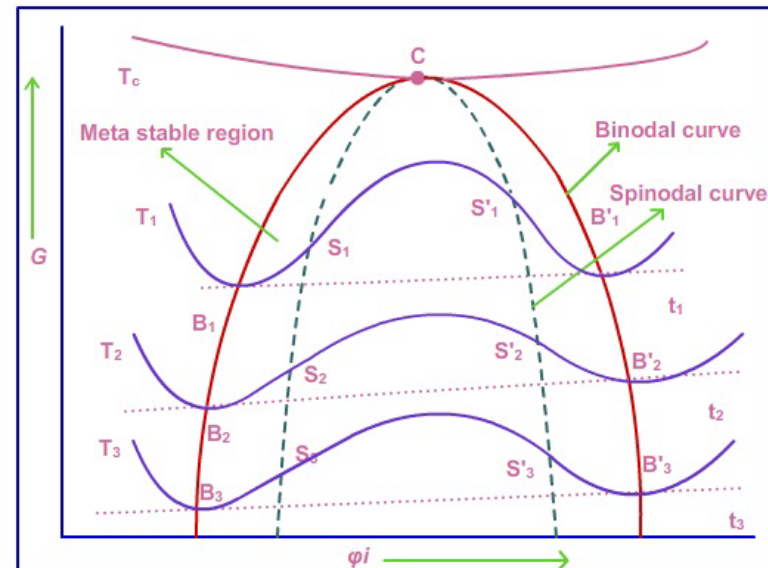
$$\frac{\Delta G}{RT} = (x_1 \ln x_1 + x_2 \ln x_2 + x_1 x_2 \chi)$$

$$\frac{\Delta H_m}{RT} = x_1 x_2 \chi$$

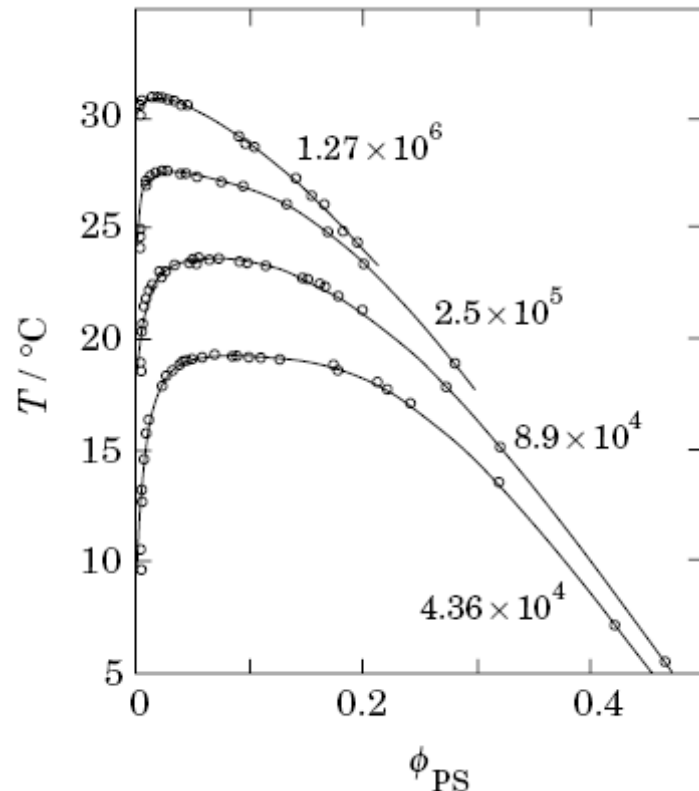
enthalpie



total miscibility requires:
 $\Delta G_m < 0$ and $\delta^2 G_m / \delta \varphi^2 > 0$



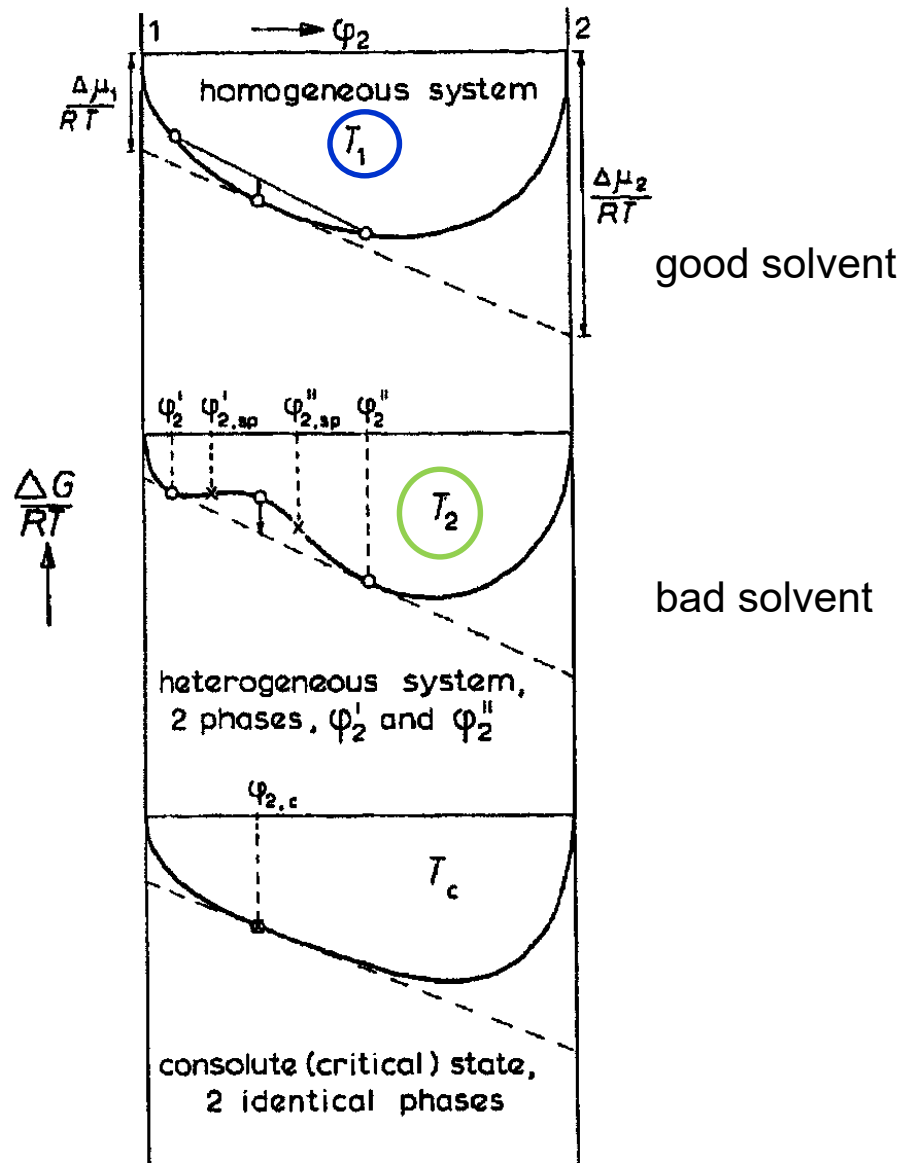
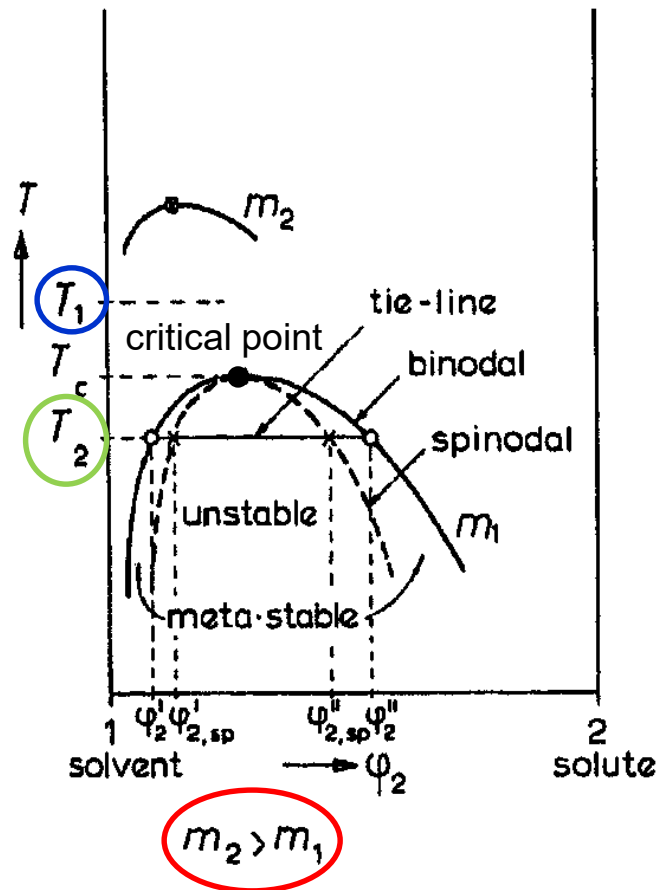
Phase Diagram of Polymer Solution



Coexistence curves determined from the cloud-point method (circles) for solutions of polystyrene of different molecular weights in cyclohexane. The abscissa is the volume fraction of PS. The MW of the polymer in g/mol is indicated adjacent to each curve.

Phase Diagram of Polymer Solution

free energy of mixing as a function
of composition in a binary liquid
system showing partial miscibility



Binodal, Spinodal and critical point

$$\frac{\Delta G}{RT} = (1 - \nu_2) \ln(1 - \nu_2) + \frac{\nu_2}{N} \ln \nu_2 + \chi \nu_2 (1 - \nu_2)$$

$p, T = \text{const.}$
 $R = k_B N_{Av}$

$N = \text{degree of polymerization}$

$$\frac{\delta}{\delta \nu_2} \left(\frac{\Delta G}{RT} \right) = 0 \quad \frac{\delta}{\delta \nu_2} \left(\frac{\Delta G}{RT} \right) = -\ln(1 - \nu_2) - 1 + \frac{\ln \nu_2}{N} + \frac{1}{N} + \chi - 2\chi \nu_2 = 0$$

$$\frac{\delta^2}{\delta \nu_2^2} \left(\frac{\Delta G}{RT} \right) = 0 \quad \frac{\delta^2}{\delta \nu_2^2} \left(\frac{\Delta G}{RT} \right) = \frac{1}{(1 - \nu_2)} + \frac{1}{N \nu_2} - 2\chi = 0$$

$$\frac{\delta^3}{\delta \nu_2^3} \left(\frac{\Delta G}{RT} \right) = 0 \quad \frac{\delta^3}{\delta \nu_2^3} \left(\frac{\Delta G}{RT} \right) = \frac{1}{(1 - \nu_2)^2} - \frac{1}{N \nu_2^2} = 0$$

spinodal: $\frac{\delta^2}{\delta \nu_2^2} \left(\frac{\Delta G}{RT} \right) = 0$

binodal: chemical potentials of both, solvent and polymer, are equal in two coexisting phases (common tangent)

critical point: $\frac{\delta^3}{\delta \nu_2^3} \left(\frac{\Delta G}{RT} \right) = 0$

Critical Point - Flory Krigbaum Equation

T_c and ϕ_c depend on polymer molecular weight

$$x_c = \phi_c = \frac{1}{1 + \sqrt{N}}$$

x_c : critical concentration at which phase separation occurs

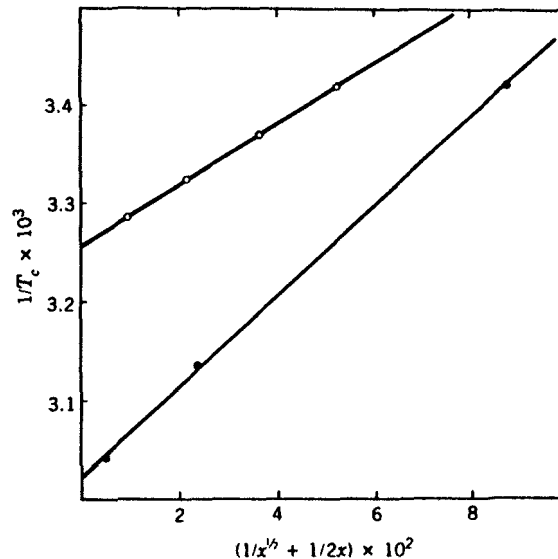
N : degree of polymerization

T_c and T_Θ : critical temperature and theta temperature

Remark: F.-H. theory does not permit volume change on mixing, ignore equation of state properties of pure comp. and enormous size differences polymer - solvent

Flory Krigbaum:

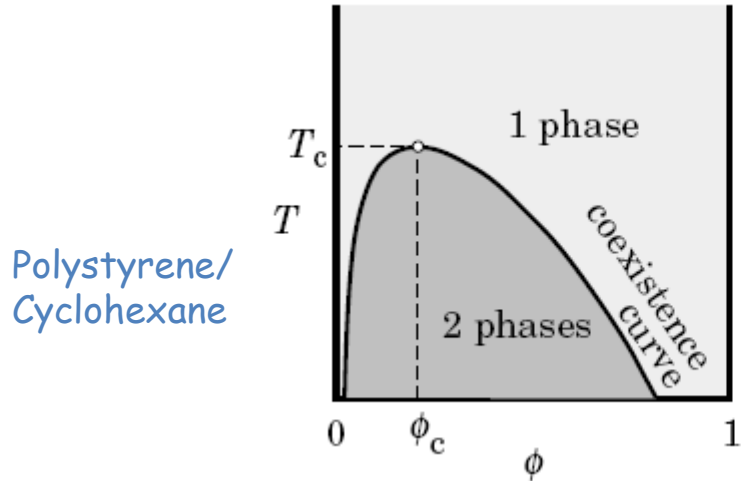
$$\frac{1}{T_c} = \frac{1}{T_\Theta} \left(1 + \frac{1}{\Psi_1} \left(\frac{1}{\sqrt{N}} + \frac{1}{2N} \right) \right)$$



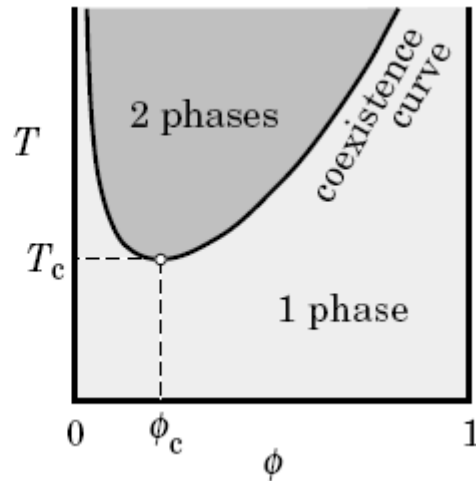
Dependence of the critical temperature on the number of segments per polymer chain.
(○) Polystyrene in cyclohexane;
(●) Polyisobutylene in diisobutylketone
A.R. Shultz, P.J. Flory; J. Am. Chem. Soc., 74, 4760, 1952.

Upper and Lower Critical Solution Temperature

UCST-type phase diagram

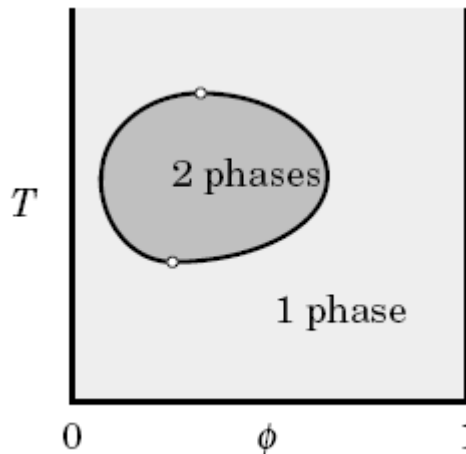


LCST-type phase diagram



Polyethylene /
Hexane (5 bar)
or
Polystyrene /
Polyvinylmethylether

Phase diagram of polymer solution on temperature-composition plane
The critical point is at the apex of the coexistence curve and is specified
by the critical temperature T_c and the critical composition ϕ_c .



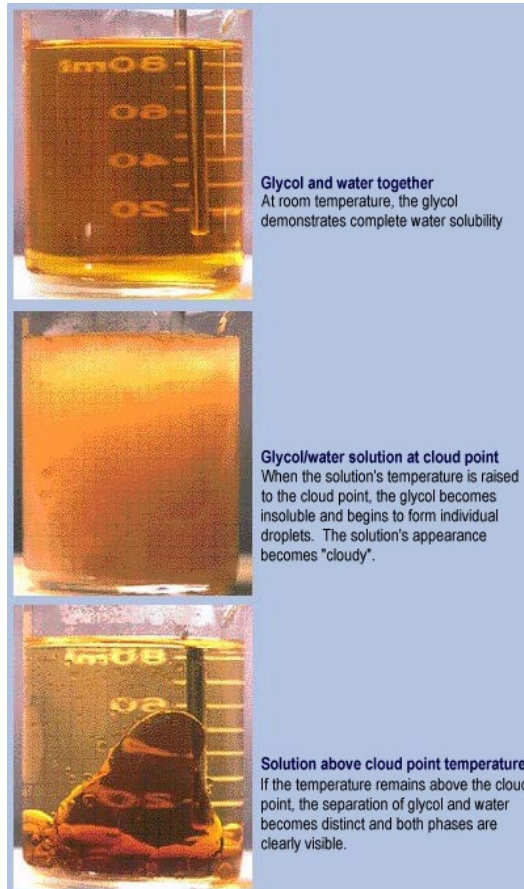
A phase diagram can show both upper and lower critical solution temperatures.

Polyoxyethylene /
Water

Measuring Phase Diagrams

Cloud point method

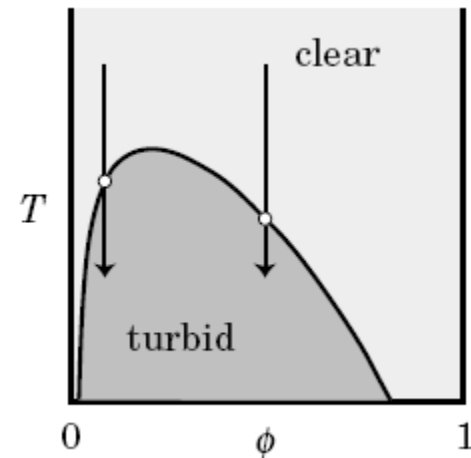
As the temperature crosses the coexistence curve, the solution becomes turbid, indicating microscopic heterogeneity. The point is called the cloud point. The turbidity is due to scattering of light by a difference in the refractive index between the two phases. When left for a sufficiently long time, the polymer–solvent system separates into two macroscopic phases, each of which is uniform and therefore transparent.



Cloud point is defined as the temperature at which the solution becomes turbid as the solution in a single phase is brought into the two-phase region.

Illustration is given for the UCST-type phase diagram.

By connecting the cloud points measured for solutions of different concentrations, we can obtain the coexistence curve and construct the phase diagram.



Applications of Phase Diagrams

Polymer fractionation represents a direct application of the Flory-Huggins theory. All synthetic polymers and the majority of natural polymers (with the exception of proteins) are polydisperse. Fractionation is used to reduce polydispersity (i.e. the width of the molecular weight distribution). Fractionation is based on variation of T_c with the polymer MW ($\propto x$). It was shown previously that T_c changes with x according to the Flory-Krigbaum equation

$$1/T_c \approx (1/T_\theta) [1 + 1/(\psi_{12}\sqrt{x})]$$

where ψ_{12} is a temperature-independent parameter specific to the couple polymer/ solvent .

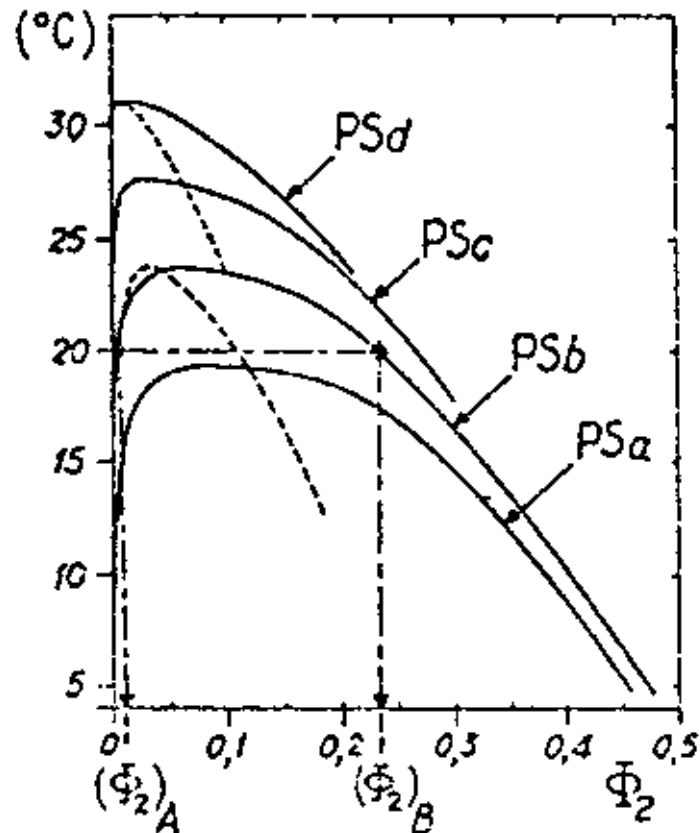
For the couple polystyrene/cyclohexane, for instance, $\psi_{12} = 1.07$ and $T_\theta = 34^\circ\text{C}$.

$$x = 389 \quad T_c = 19.8^\circ\text{C}, (\chi_{12})_c = 0.552, (\Phi_2)_c = 0.048$$

$$x = 757 \quad T_c = 23.8^\circ\text{C}, (\chi_{12})_c = 0.537, (\Phi_2)_c = 0.035$$

$$x = 2110 \quad T_c = 28.0^\circ\text{C}, (\chi_{12})_c = 0.522, (\Phi_2)_c = 0.021$$

$$x = 12450 \quad T_c = 31.5^\circ\text{C}, (\chi_{12})_c = 0.509, (\Phi_2)_c = 0.009$$

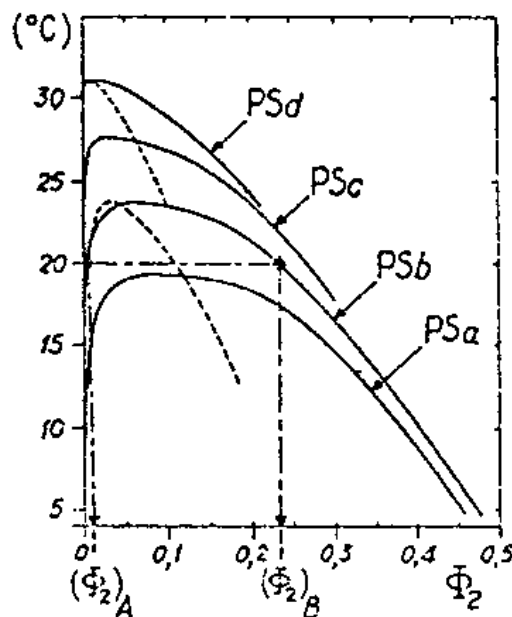


Experimental demixing curves for 4 fractions of PS in cyclohexane.

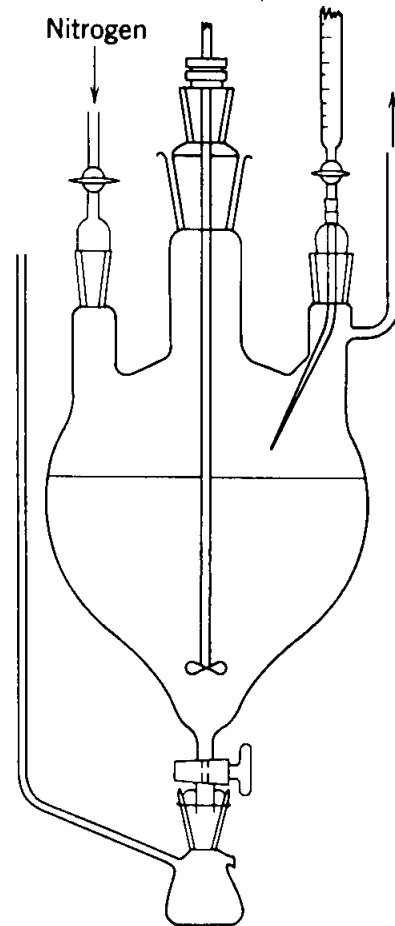
PSa : $x = 389$, PSb : $x = 757$, PSc : $x = 2110$, PSd : $x = 12450$. Dotted lines : theoretical prediction.

Preparative Fractionation

Let us suppose that a polymer solution contains initially 3.5% vol. of PS with a MW of 78'700 ($x = 757$) and 4.8% vol. of PS with a MW of 40'500 ($x = 389$) in cyclohexane. By cooling the solution from 24°C to 20°C, the highest MW fraction precipitates while the lowest MW fraction remains in solution. By this procedure, we have separated the mixture into two fractions of different MW. The separation is not quantitative, however. By tracing an horizontal line at 20°C on the demixing curves, it can be determined that the concentration of the PS-78'700 in the polymer-rich phase is ~23%, while ~1% still remain in solution.



Experimental demixing curves for 4 fractions of PS in cyclohexane.
PSa : $x = 389$, PSb : $x = 757$, PSc : $x = 2110$, PSD : $x = 12450$. Dotted lines : theoretical prediction.



Polymer – Polymer Systems

Case 3 of lattice model: reduced combinatorial entropy of mixing

$$\frac{\Delta G_m}{RT} = \underbrace{\frac{\nu_A}{N_A} \ln \nu_A + \frac{\nu_B}{N_B} \ln \nu_B}_{\text{Entropic term}} + \underbrace{\chi \nu_A \nu_B}_{\text{Enthalpic term}}$$

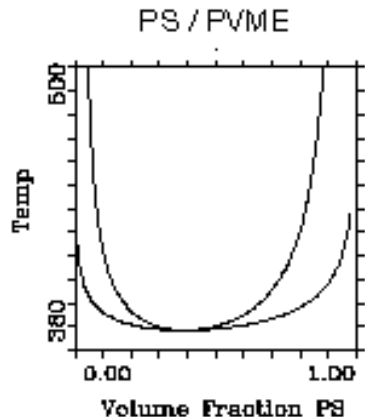
ν_A / ν_B : volume fraction
 N_A / N_B : degree of polymerization
of polymer A and B resp.

- Homogenous blends = solution of polymer A ($N_A \gg 1$) in polymer B ($N_B \gg 1$)
- The possible arrangements of the monomers of polymer B are reduced by polymer A:
 ΔS_m (blends) $<$ ΔS_m (polymer/solvent) but still positive.
- In the case of a symmetric polymer blend ($N_A = N_B$) the critical composition $\nu_{A \text{ crit}} = \frac{1}{2}$.
For infinite molecular weight $N \rightarrow \infty$ the interaction parameter $\chi_{\text{crit}} = 0$.
- In contrast to a blend, a polymer solution where $N_B = 1$ (solvent) the critical composition $\nu_{A \text{ crit}} = 0$ and $\chi = \frac{1}{2}$.
- $\chi_{\text{crit}} \rightarrow 0$ for polymer blend because the entropic contribution to the free energy of mixing is very small, in first approximation the entropic term can be thought of as zero. This corresponds to the fact that only very few miscible polymer blends exist.

Phase separation and dissolution are controlled by T, p and c

UCST and LCST in Phase Diagrams of Polymer Blends

phase diagram with LCST



phase diagram with UCST

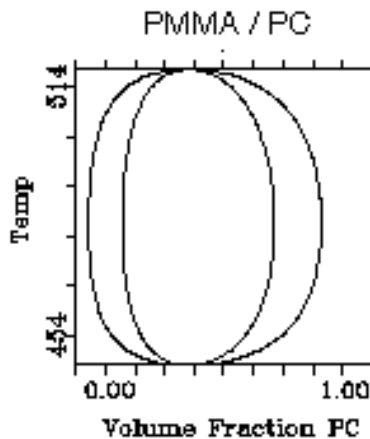
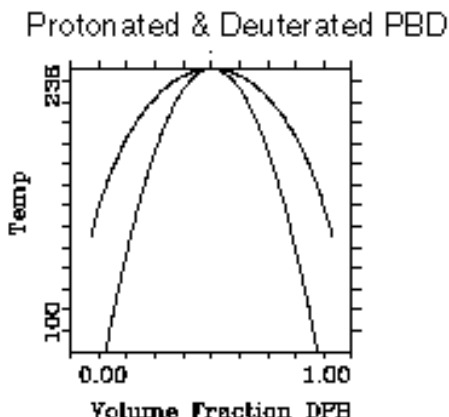
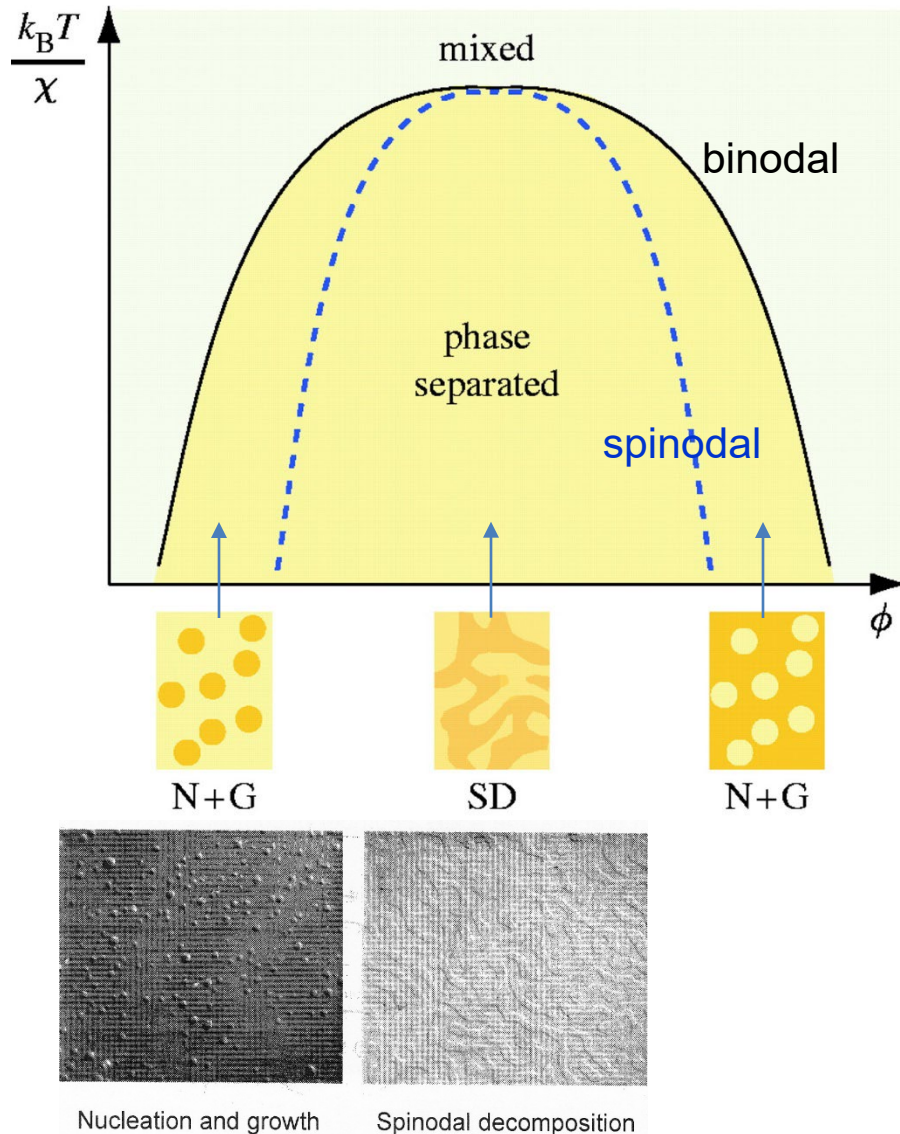


diagram with LCST and UCST

Kinetics of Phase Separation

How the phase separation occurs?



Considering a homogeneous system out of its region of stability

2 processes are observed:

Spinodal Decomposition

Nucleation and Growth

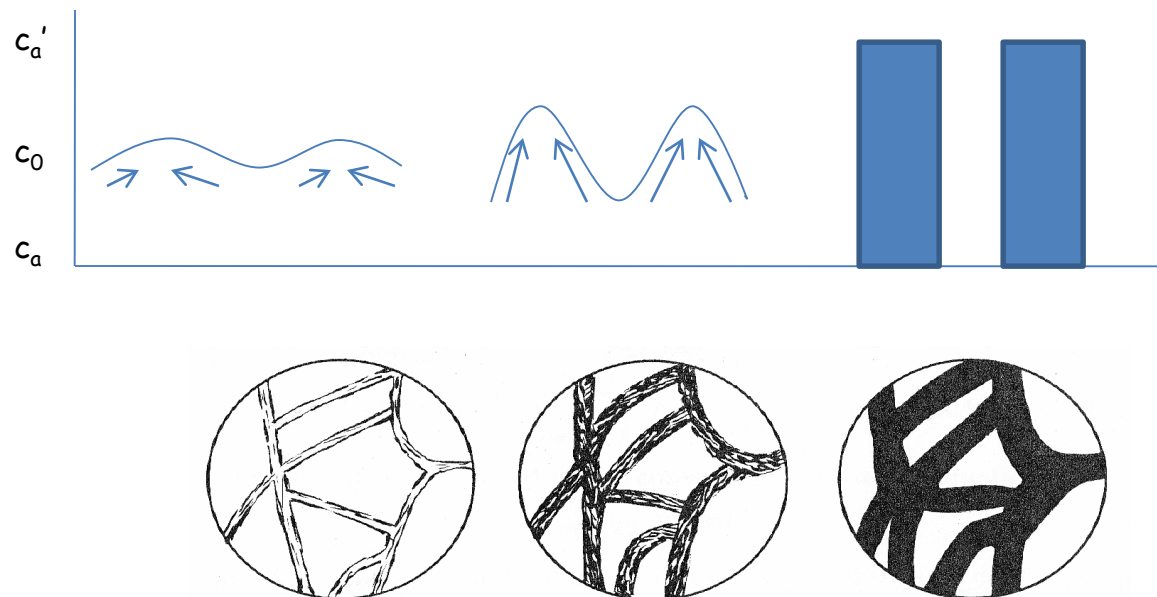
Phase Separation: Spinodal Decomposition

The homogeneous system beyond the spinodal curve, with $\frac{\delta^2 G}{\delta \phi^2} < 0$, is unstable with respect to any infinitesimal concentration fluctuation, and any such fluctuation grows with time leading to the process of so-called spinodal decomposition.

If there happens to be a region rich in polymer, the polymer starts diffusing into this region, thus increasing the fluctuation until the equilibrium volume fraction of a new phase is reached.

Thus, the amplitude of wavelike composition fluctuations increases with time. And, there rapidly arises a pattern of interpenetrating domains with concentrations with c_a and c_a' .

Unstable process; no activation energy required.



Phase Separation: Nucleation and Growth

Consider now the case when the homogeneous phase is not stable anymore but $\frac{\delta^2 G}{\delta \phi^2} > 0$.

This indeed happens if the state in question lies between the binodal and the spinodal curves (metastable region). The small concentration fluctuations are still suppressed.

To initiate the phase separation a fluctuation exceeding some critical size (in both terms of the concentration difference and in terms of the spatial extent). These extremely large fluctuations act as nuclei for the new phase which starts to grow around them.

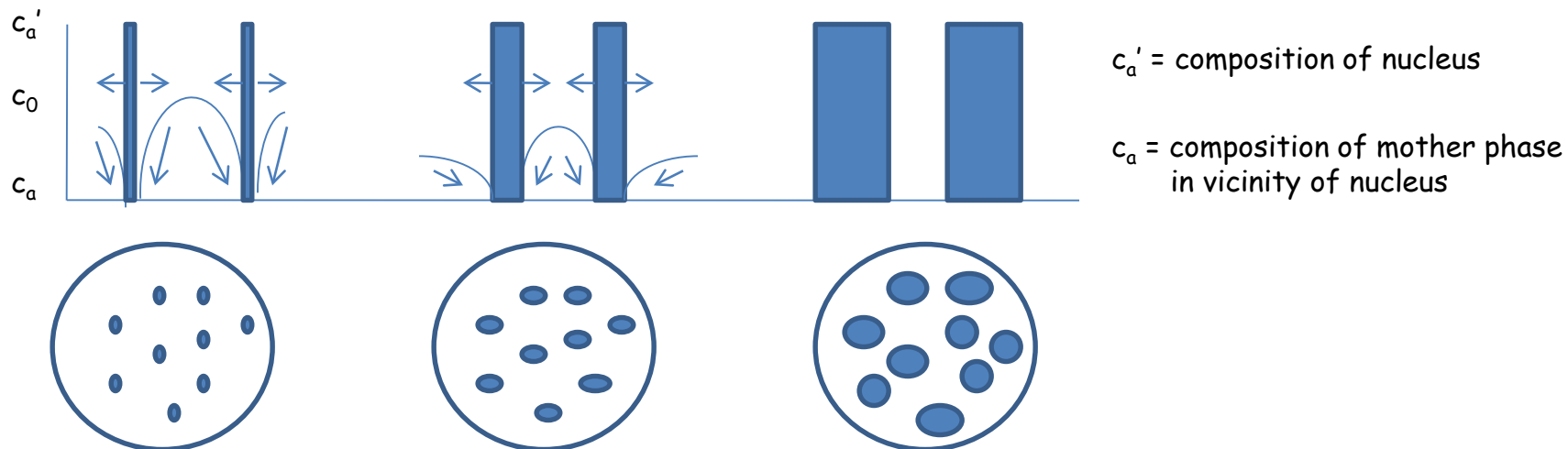
Nucleation: generating an initial fragment = nucleus

formation of nucleus requires an increase of free energy

2 contributions to free energy:

1. work spent in forming the surface
2. work gained in forming the interior

Required activation energy, process is much slower than the spinodal decomposition, since large fluctuations are extremely rare.



Example of Spinodal Phase Separation

Polystyrene-blend-Poly(vinylmethylether)

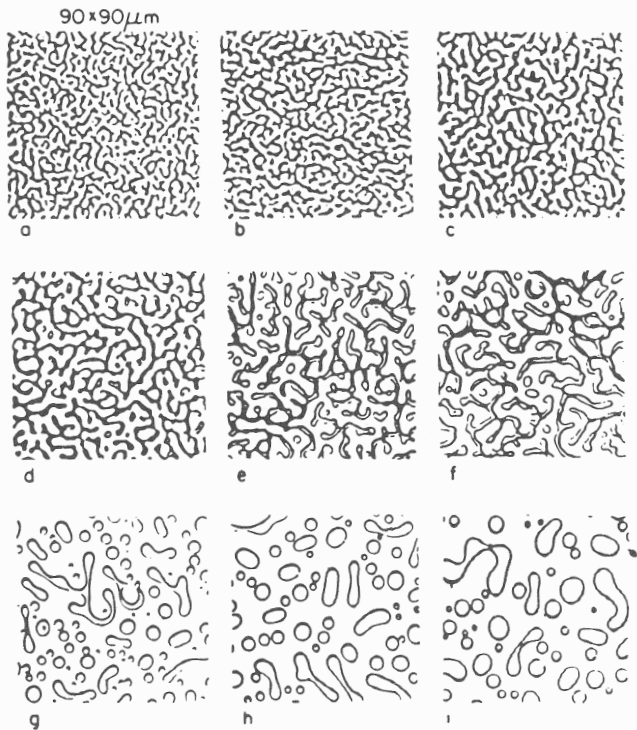


Figure 4.10 Coarsening during the latter stages of spinodal phase separation polystyrene-blend-poly(vinyl methyl ether).

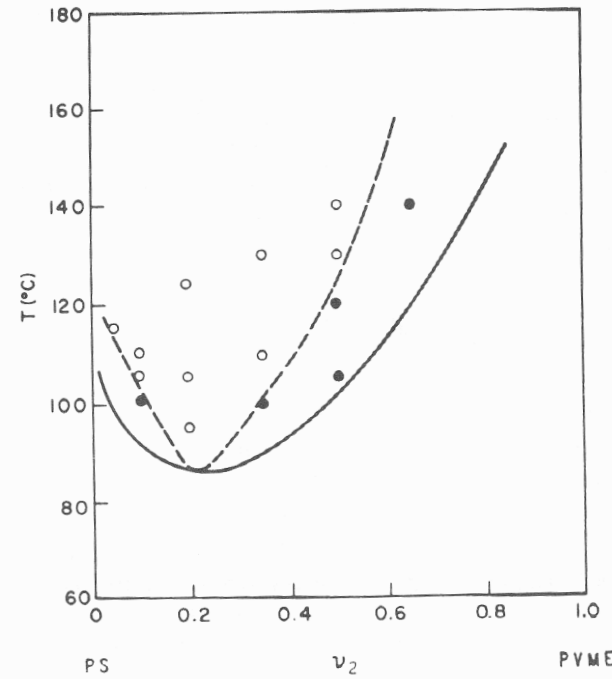


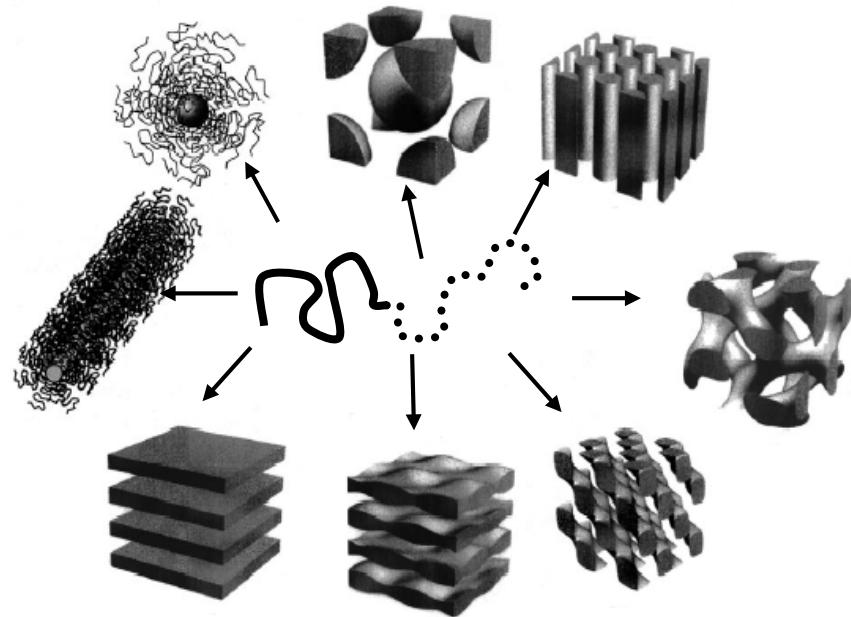
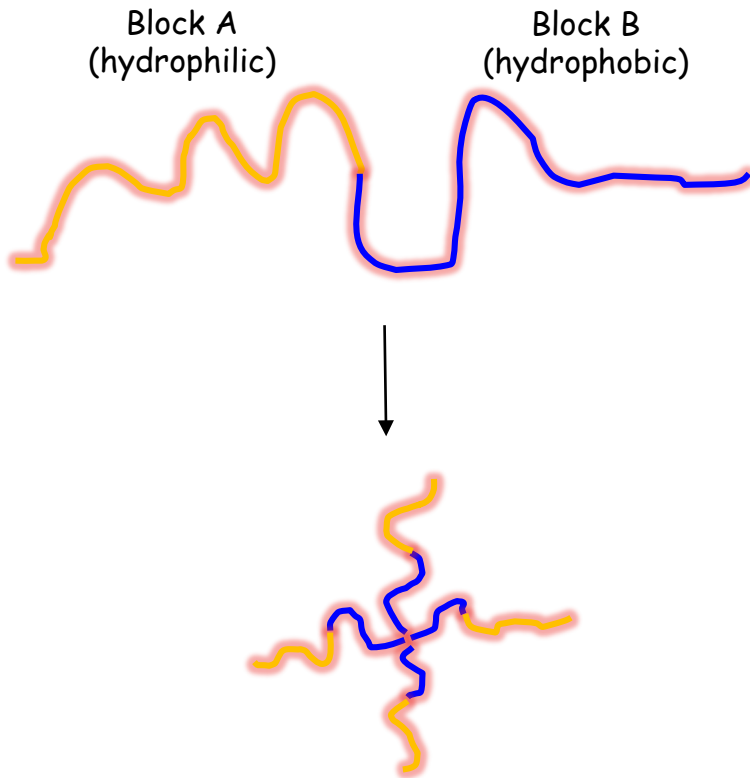
Figure 4.11 Phase separation by spinodal decomposition (○) and nucleation and growth (●), as observed under a microscope (35).
taken from L.H. Sperling

Summary of Polymer Solutions

1. Thermodynamic arguments were also sufficient to show how the complete phase diagram (T, ϕ) for a binary system could be constructed from an expression for the free energy of mixing. The key features of the phase diagram are the critical point, the coexistence curve (binodal), and the stability limit (spinodal).
2. Developing an expression for the free energy of mixing based on the Flory-Huggins Theory.
3. The Flory Huggins model was explored in detail, in terms of its predictions for B (or A_2 Virialcoefficient) and for the phase diagram.
4. The concept of a theta solvent emerges as a central feature of polymer solutions
It has four equivalent operational definitions:
 - (a) the temperature where $B = 0$,
 - (b) the temperature where the interaction parameter $\chi = 1/2$.
 - (c) the limit of the critical temperature T_c as $M \rightarrow \infty$.
 - (d) a solvent in which $R_g \sim M^{1/2}$.

Physically, a theta solvent is one in which the polymer-solvent interactions are rather unfavorable, so that the chain shrinks to its random walk dimensions. This contractions cancels the effect of the excluded volume interactions, which otherwise swells the chain to self avoiding conformations: $R_g \sim M^{3/5}$.

Outlook: Block Copolymer Phase Behavior



S. Förster, T. Plantenberg *Angew. Chem. Int. Ed.* **2002**, *41*, 688

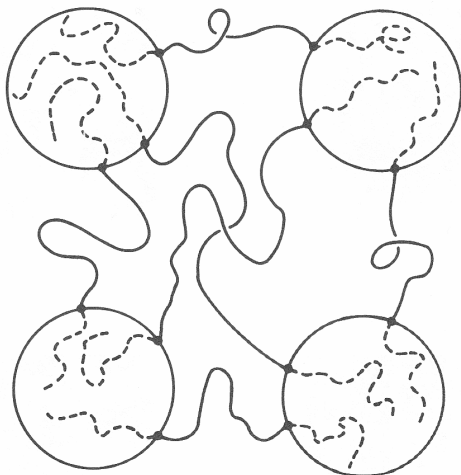
Block copolymers are interesting because they can self-assemble in a variety of ways. Knowing under what conditions specific phases (or structures) are obtained is necessary for the use of such materials in real-world applications.

Morphology of Block Copolymers

Block copolymers are miscible to higher block molecular weight than their corresponding blends.

Question: If block copolymers phase separate, how big are the domains?

domain = discrete region of space occupied by one phase and surrounded by another



Elastomeric block
 Glassy or crystalline block
 Block copolymer junction

Depending on the relative length of the two blocks, the morphology of the phases changes

Spheres → Cylinders → alternating Lamellae

short – long

about the same length

Figure 4.16 Idealized triblock copolymer thermoplastic elastomer morphology.

Example: polystyrene – block – polybutadiene – block – polystyrene used as rubbery shoe sole material
long, rubbery center block forms the continuous phase whereas the short, glassy PS block form submicroscopic spheres

Morphology of Block Copolymers

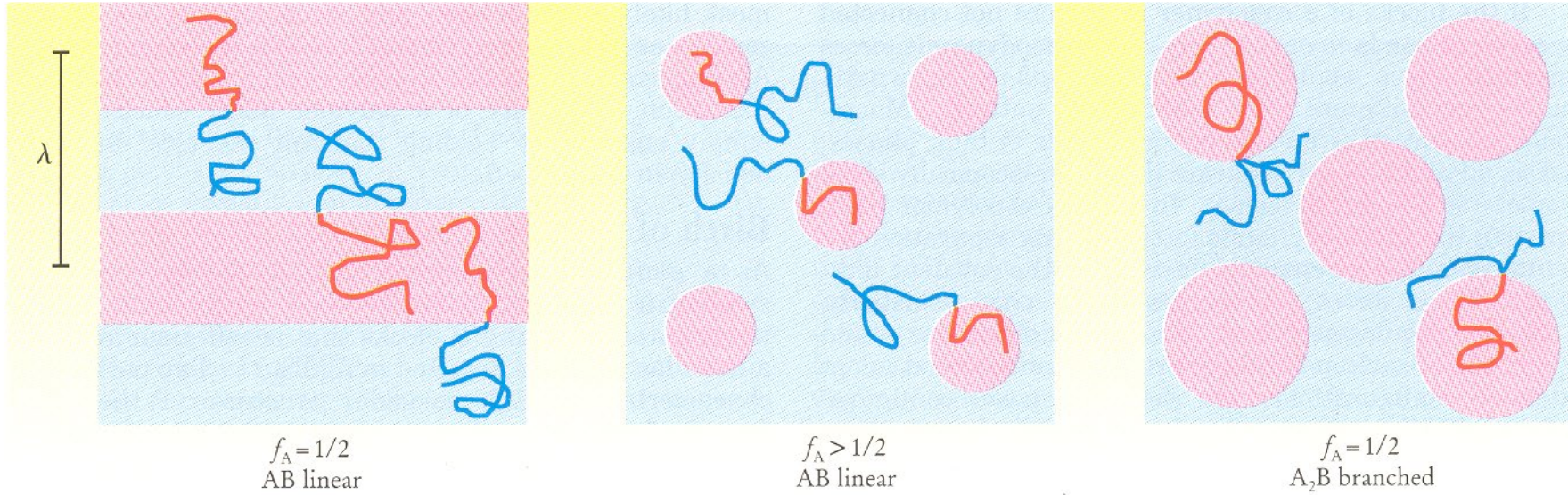
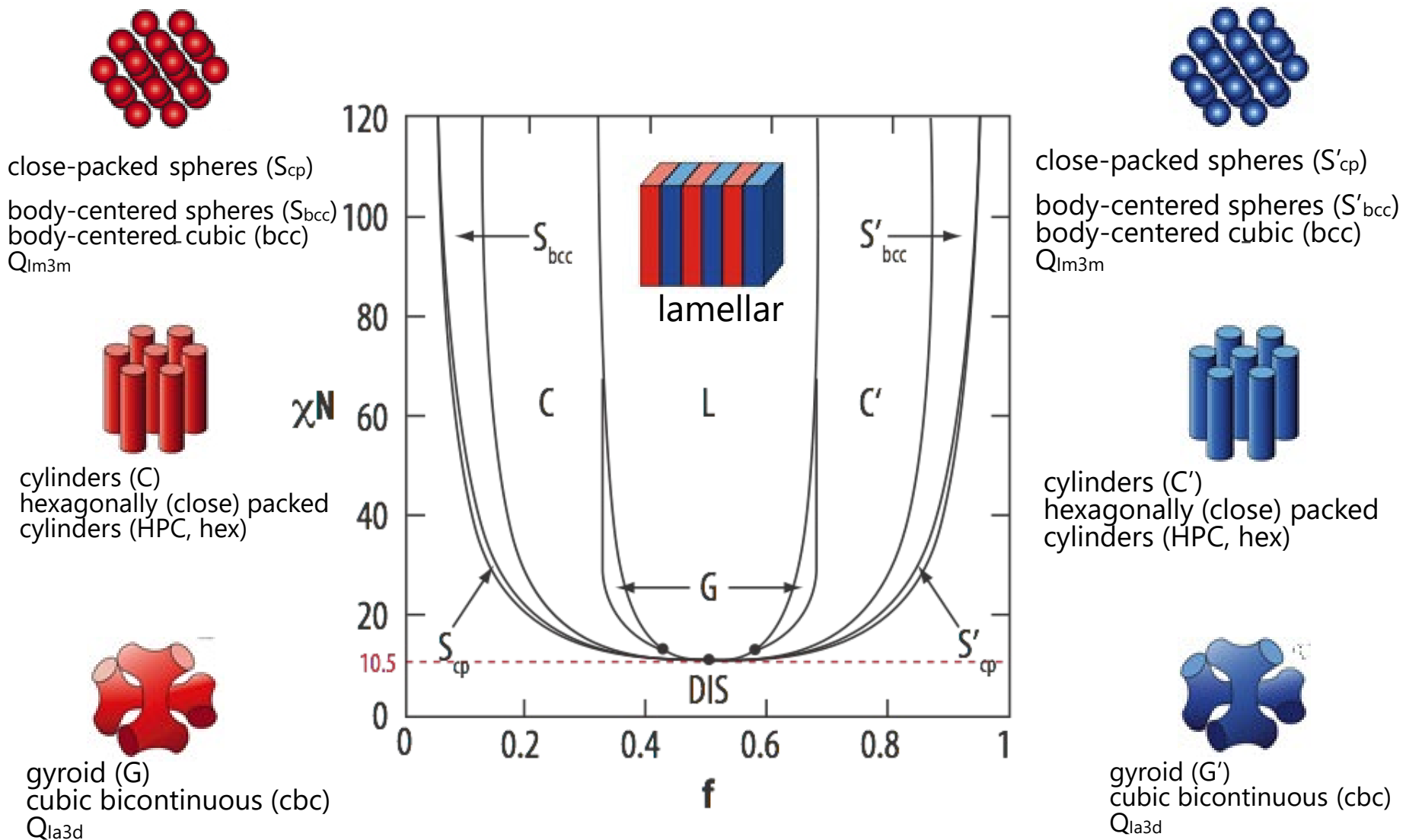


FIGURE 2. DIBLOCK MORPHOLOGY depends on block composition. Interfacial curvature of block copolymers can be controlled by adjusting the composition f or changing the molecular architecture. Shaded regions are block-segregated microdomains colored according to monomer type, with blue for type A and red for type B monomers. **a:** Self-assembly of symmetric ($f_A = f_B = 1/2$) linear AB diblocks leads to a lamellar morphology. **b:** Increasing the volume fraction of one block (in this case, $f_A > 1/2$) induces interfacial curvature, resulting in a nonlamellar morphology, such as cylindrical or spherical. **c:** A branched A_2B architecture can result in a nonlamellar morphology even in a compositionally symmetric molecule, due to asymmetric interfacial crowding.

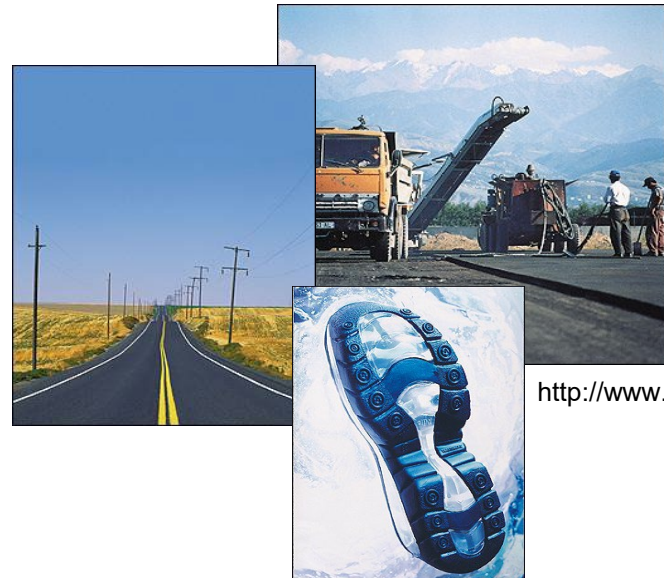
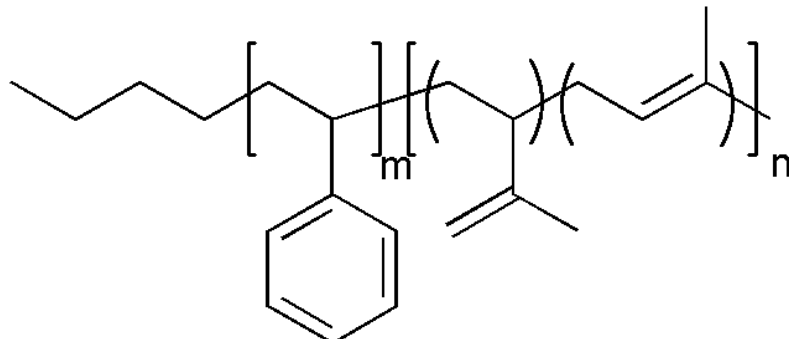
Theoretical AB Diblock Copolymer Phase Diagram



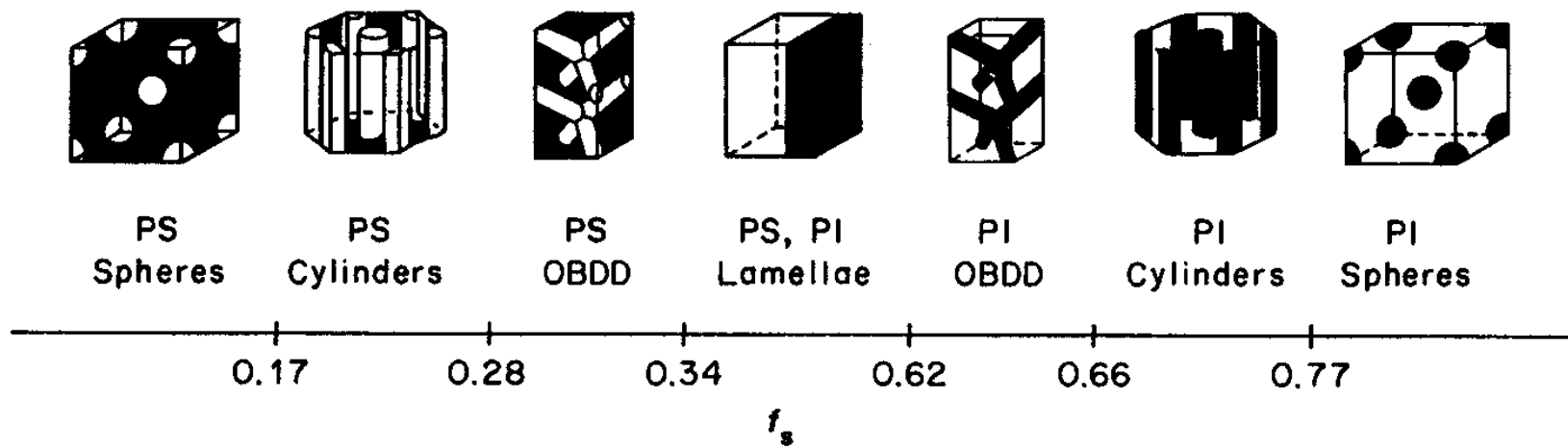
Bates, Macromolecules 1996, 29, 7641. Science 1991, 251, 898; Phys. Today 1999, 32.

Example of Diblock Copolymer

Polystyrene-b-polyisoprene



Phase Diagram



27²⁷

Phases of PS-PI Block Copolymers

Transmission Electron Microscopy (staining with OsO₄)

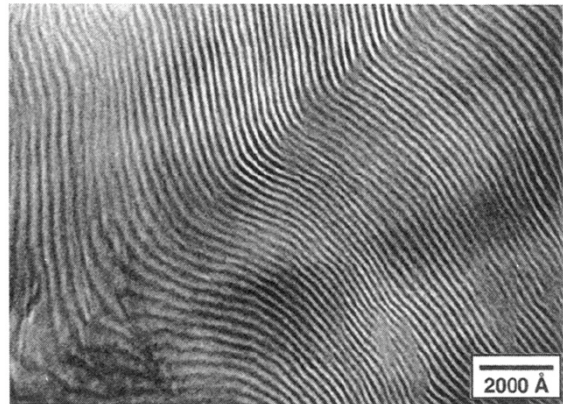


Figure 3. TEM micrograph from sample IS-68. The sample was annealed at 120 °C for about 5 h in vacuum and subsequently quenched in liquid nitrogen. A lamellar microstructure is assigned to phase A based on this and other similar results.

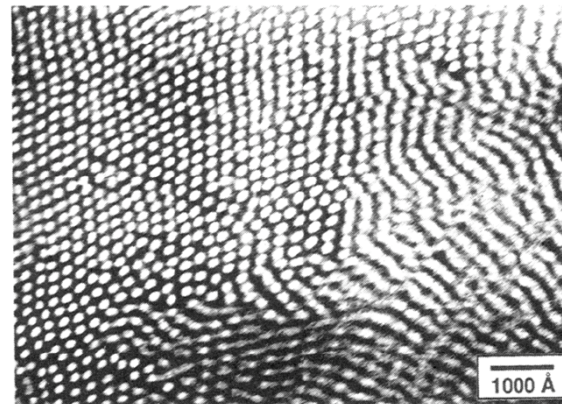


Figure 4. Representative TEM micrograph obtained from sample IS-68 after annealing at 260 °C for 2 h followed by quenching in liquid nitrogen. Hexagonally packed cylinders of polystyrene in a polyisoprene matrix have been associated to phase C based on this and other similar micrographs.

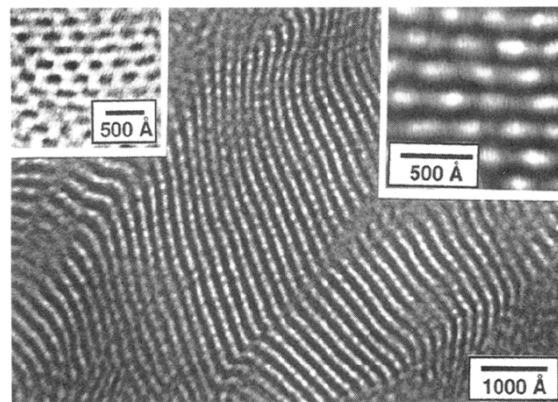


Figure 5. A commonly observed projection of the microstructure associated with phase B. Regions showing a "wagon wheel" type of morphology can be seen in this micrograph. The sample was IS-68, annealed at 220 °C for 3 h followed by a liquid nitrogen quench. Based on SAXS and SANS analysis, we have identified this as the bicontinuous *Ia*³*d* morphology.

Small Angle Neutron Scattering

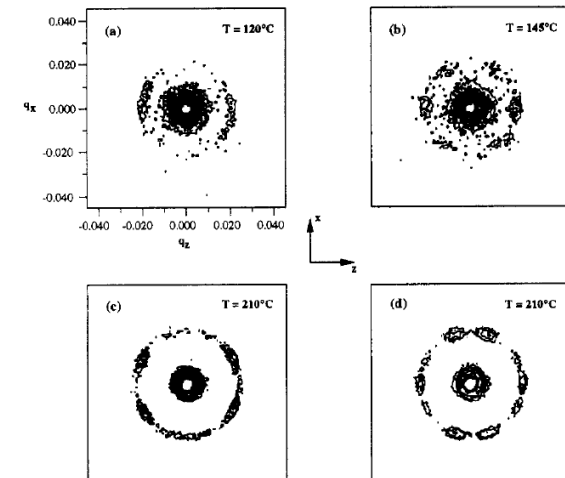


Figure 10. Contour plots of SANS patterns for the sample IS-68 in three different ordered states (A, D, B). A nearly featureless pattern (a) was observed in state A (120 °C), which is attributed to a parallel orientation of lamellae with respect to the shear plane. After heating the sample to 145 °C (state D) and application of dynamic shearing ($\dot{\gamma} = 0.1 \text{ s}^{-1}$ with $|\dot{\gamma}| = 300\%$), a weak hexagonal scattering pattern was observed (b). This is consistent with a hexagonal in-plane arrangement of perforations in the minority (PS) layers. Further heating the sample to 210 °C, without shear (state B), produced a predominantly four-peak pattern (c), which transformed into result (d) when a shear rate of 2.2 s^{-1} was applied. The azimuthal relationship between the combined 10 reflections in (c) and (d) is consistent with the SANS data reported for sample IS-39 (ref 22) and the *Ia*³*d* space group symmetry.

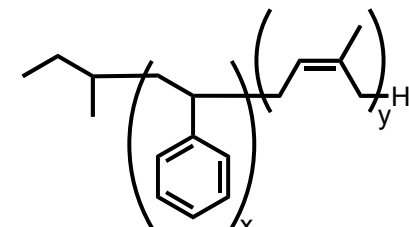
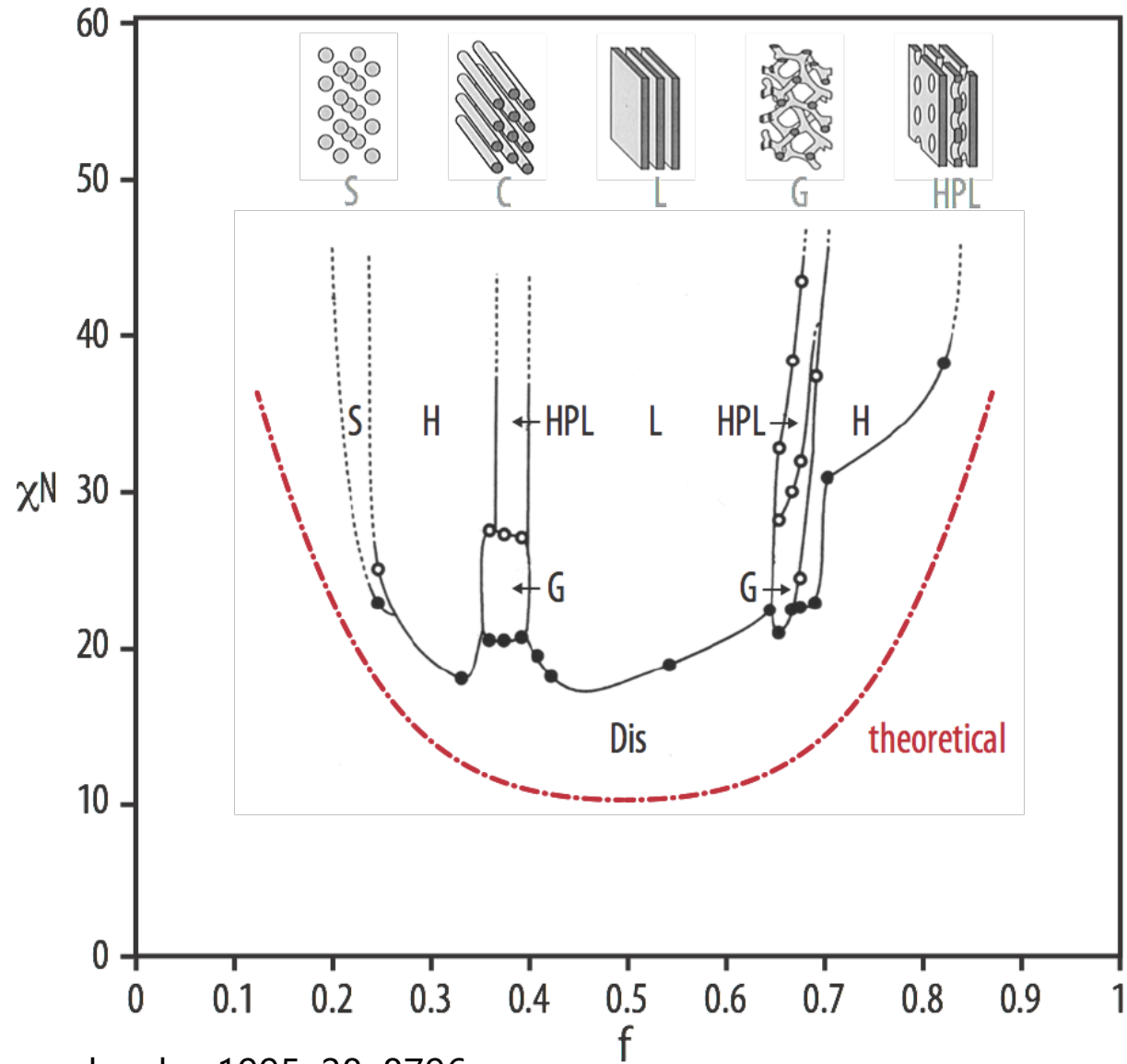


Figure 6. Representative projections of state D taken from sample IS-68 after annealing at 145 °C for 6 h followed by quenching in liquid nitrogen. Alternating light (PS) and dark (PI) layers are observed with perforations in the minor (PS) phase. The inset of the right provides a magnified view of this perpendicular orientation while the one on the left illustrates a section of the sample lying parallel on the microscope stage. In the latter, a hexagonal arrangement of PI perforations in the PS layer can be seen. Phase D is associated with the HPL morphology.

Phases of PS-PI Block Copolymers



Morphology of Tri-Block Copolymers

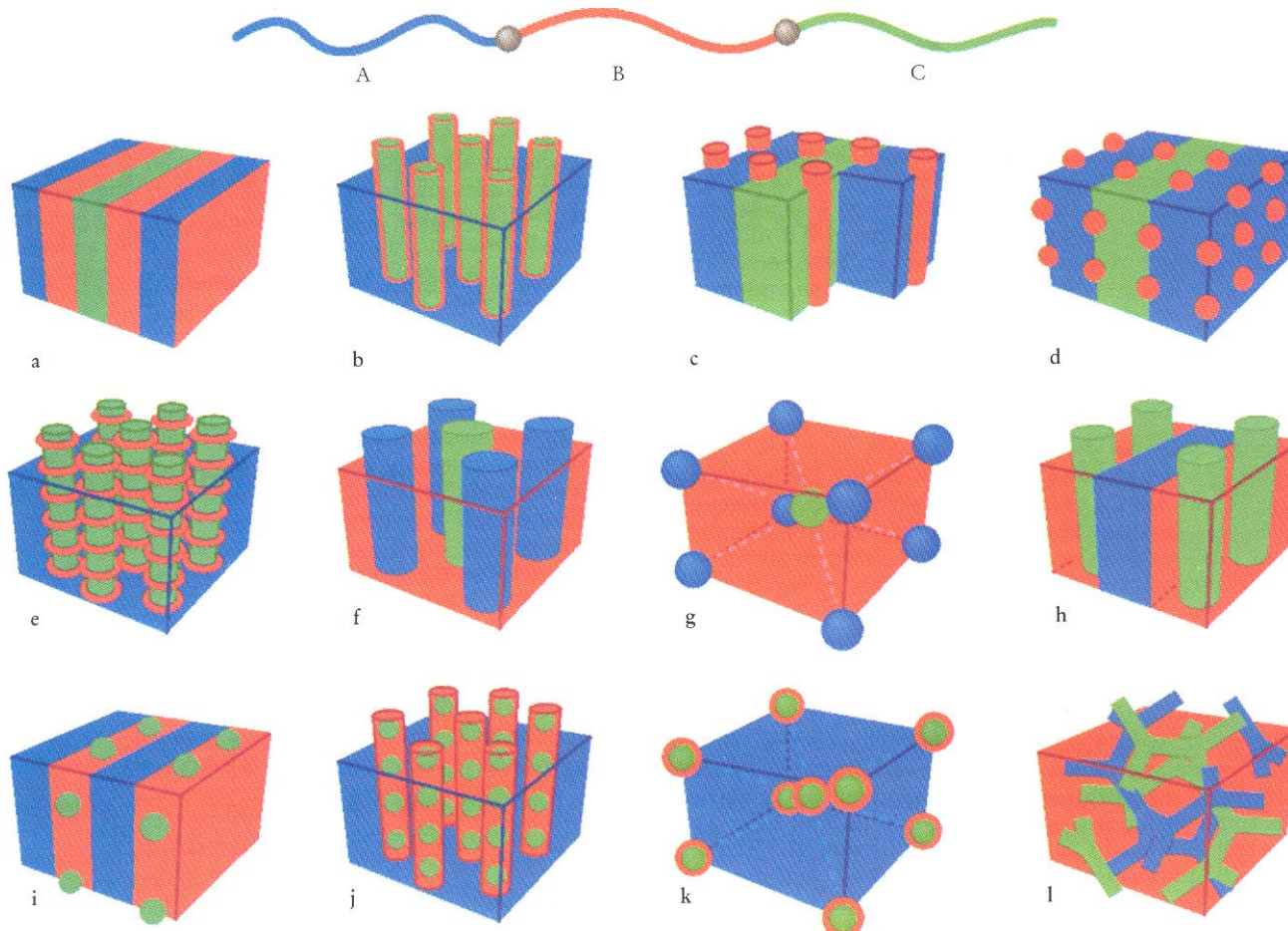


FIGURE 5. MORPHOLOGIES FOR LINEAR ABC triblock copolymers. A combination of block sequence (ABC, ACB, BAC), composition and block molecular weights provides an enormous parameter space for the creation of new morphologies. Microdomains are colored as shown by the copolymer strand at the top, with monomer types A, B and C confined to regions colored blue, red and green, respectively. (Adapted from Zheng and Wang in ref. 13.)